Paper ID: MS-12

Effect of Cu Composition & Ageing Treatment on Inherent Property Development of AA2024

Naharin Jannath and H M Mamun Al Rashed

Department of Materials and Metallurgical Engineering, Bangladesh University of Engineering and Technology, Dhaka 1000, Bangladesh

E-mail:hrashed@mme.buet.ac.bd

Abstract

AA2024 is a popular aerospace alloy used widely in fuselage, wing & fittings of airplanes due to its high strength to weight ratio. Copper (Cu) is one of the major alloying elements of this alloy. In this work, changes of microstructural properties were observed by varying Cu content. Alloys were cast containing different amount of Cu in the common AA2024 alloy. Thermodynamic modelling of the alloys predicted the phase fractions of the alloys and also the appropriate homogensition temperature. After homogenisation at the defined temperature, DSC was carried out to understand the kinetics of precipitates. The peaks of the DSC curves were also compared with the modelling results to obtain information about the type of the particles. Careful observation of DSC results confirmed the presence of the particles. SEM investigation of the alloys were carried out to identify the second phase particles, followed by image analysis to calculate the volume fractions of the particles. The results matched closely with the modeling data. The alloys were also observed under optical microscope. it was found that increasing the amount of Cu increased the number of precipitates at large in the microstructure, and so particles per unit area was also increased. Their orientation is almost aligned in a particular direction just beneath the skin. However, at the centre of cast product, the colony of particles was fragmented and distributed randomly. Particle size was also varied with distance. Two major phases were clearly identified optically. Grain size of the alloys were also measured. Cu appeared to modify microstructure profoundly by both contributing to changes in grain size, and amount of second phase particles and their distribution. Capability of microstructure evolution with sizable modeling data provides a great advantage in understanding, and optimizing of the process parameters.

Keyword: Aluminum alloy, microstructure, ageing, hardness

Introduction

High strength in age harden able alloys is caused by Precipitates. The major alloying elements in the AA2024 containing copper and magnesium. The major precipitates in this alloy are Al and Al2Cu. The basis of hardening is the formation during the decomposition of the supersaturated solid solution (SSS) of one or more metastable transition phases prior to the equilibrium precipitate. These precipitates develop sequentially, with increasing time at temperature between room temperature and the solvus. In the binary Al-Cu system, the three stages are identified as;

$$\text{SSS - GP I – GP II}(\theta'') – \theta' - \theta(CuAl_2)$$

GP 1 phase is a zone structure and forms immediately at room temperature as plate like copper rich regions on the (100) planes of the aluminum rich matrix [1]. They are reported to be 30-50Å in diameter and 100Å apart. On raising the temperature above 100°C, the GP I zones are replaced by the GPII or θ'' zones. Structurally, they are similar to GP I zones except bigger. They also lie on the (100) plane and are coherent in the aluminum matrix [2, 3]. On further raising the temperature, the θ” grows and the coherency with the matrix breaks and this leads to the formation of dislocation rings. It is at these rings that the semi coherent θ' nucleate and grow at the expense of the θ’’ The semi coherent θ' platelets are approximately 250Å thick and lie parallel to the (100) plane. The final stage is the transformation of the θ' into the non-coherent equilibrium θ ($CuAl_2$). The θ nucleates at the θ'/matrix boundaries and consumes the θ' platelets at which it is nucleated. All three precipitate phases are reported to have tetragonal structures.

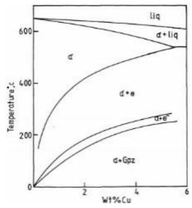

Fig. 1. Portion of Al-Cu Phase Diagram

When the Al-Cu-Mg systems with Cu: Mg ratios of 2.2:1 and 7:1. At a ratio of 2.2:1, the ageing sequence

$$SSS - GPB - S'(CuMgAl_2) - S$$

The formation of the GPB zone is not fully understood but it is known to be stable at temperatures up to 260°C with smaller lattice strains than the GP 1 zone [15-18]. The transitional phase S"(GPB) is analogous to the S" of the Al-Cu system, and the semi coherent S' ($CuMgAl_2$) consists of platelets coherent in the (021) aluminum matrix plane. The equilibrium S phase is orthorhombic and incoherent with the matrix. On further ageing the GP1 zones were succeeded by θ" and θ' precipitates, while the GPB zones were persistent throughout the ageing sequence. Peak hardness was associated with partially coherent θ' and the subsequent limited over ageing at these temperatures was controlled by the slow growth of these particles.

Experimental procedure

The alloy was made in crucible furnace. Two batches of alloys where each batch contained three alloys with different compositions of Cu.1st sample contains 3 wt.% Cu, 2nd sample had 3.5% and 3rd sample had 4.5 wt.% Cu. The main reason for making 2 batch alloys is to test each batch with different aging temperature. Each alloy is produced in crucible furnace. Then a mold of dimension 9” x 1” x 5” inches were cleaned to solidify the liquid alloy. This alloys were machined and made 3 small blocks of 75.30 cm3 volume. microstructure was observed in this stage using I scope (Model LS1053 plus). Chemical composition was analyzed by Optical Electron Spectroscopy machine. Hardness was measured using Vickers hardness tester (Model VM - 50) Then these blocks were homogenized at 450℃ for 21 hours using ProTherm Furnace (Model PLF110/30). Then they were left in the same furnace for solid solution treatment at 493℃ for 30 minutes. They were quenched at ice water bath within 15 seconds for 30 minutes. Next they were cold rolled in rolling machine and 40% thickness was reduced in several passes. The final thickness of samples were 9.9 mm. 3 rectangular samples with 10 mm diagonal were cut, grinded, rubbed with 120 to 1500 grade emery papers, polished in wheel at 300 rev/min. they were cleaned with ethanol, etched with Keller’s reagent (2ml HF (48%) + 3ml HCl + 5ml HNO_3 + 190ml H_2O) and tested under FESEM with EDS to understand quantitative properties. Then the samples were left in furnace for 5 hours for ageing. Again observed under FESEM and all microstructural data were compared, analyzed and conclusion was drawn.

Results and Discussion

Table 1 shows the obtained compositions of the three alloys.

Table 1. Results of chemical analysis in optical spectroscopy for 3 different samples AA2024

Element	Al	Cu	Mg	Mn	Fe	Si	Zn	Ni	Ca	Pb
Sample 1	94.6371	3.48	0.999	0.54	0.145	0.0391	0.126	0.0126	0.0112	0.0110
Sample 2	94.2055	4	1.000	0.55	0.163	0.0395	0.0063	0.0063	00155	0.0097
Sample 3	93.7362	4.5	0.999	0.55	0.124	0.0377	0.04	0.045	0.0073	0.0005

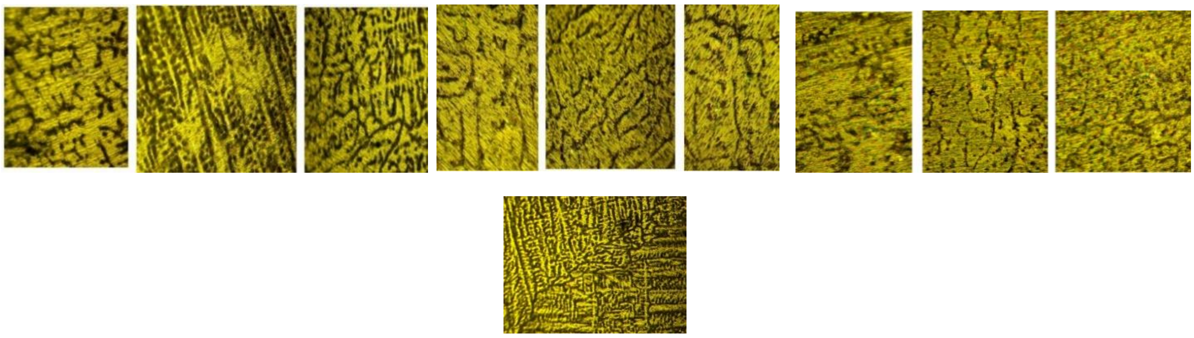

Fig. 2. As received structure of AA2024 sample 1 (1-3), sample 2 (4-6), sample 3 (7-9) & Grains (pic 10) (200x)

Microstructures of Figure 2—4 are represented for three samples of AA2024 alloy with increasing Cu wt.% spontaneously. In the as received condition, most of the structures have high angle grain boundaries (measured grain boundary angle in most cases to be $>15^{o}$) [4]. Although deformation occurs by the movement of dislocations, at large strains in materials of high-stacking fault energy, such as aluminum alloys, most of the dislocations are assimilated by dynamic recovery into LAGBs, which form a three-dimensional network of subgrains within the grains, and relatively few free dislocations are found in the sub grain interiors. To a first approximation, therefore, the microstructure of a highly deformed metal may be described in terms of the distribution of the grain and the sub grain boundaries. Small cellular dendrite is visible. Average length of these tubular phase is 25 microns. Although circular phases are present which sometimes coalesce with linear phases. They are 3 micron size precipitates with average distance of 20-35 micron distance. From edge to center, tubular structures break down and they are distributed homogeneously across the dot phases. Identification of the phases are done in FESEM/EDS section. Sample 2 and 3 have increasing amount of Cu which brought trivial changes. Specially dot phases no longer sit aside tubular phases. Linear phases are broken. It was found that average grain size became 10 microns (sample 2) from 25 microns (sample 1). Number of precipitates increase and appearance of mixed phases in more acute in sample 3 as shown in Fig. 3. Showing how dispersed phases are throughout the specimen. Precipitates are smaller and average grain size is below 7 microns. The surface and core show no significant change in distribution. After aging, microstructure changed gradually. It might the reason that aging at 190^{o} C for 5 hours causes change in mechanical properties.

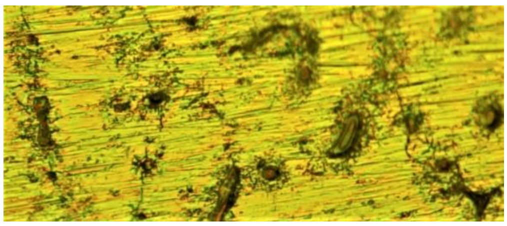

Fig. 3. Presence of colonial phases in optical microscopy (500x)

Analyzing three samples in FESEM, the presence of 7 phases were confirmed. They are provided in Table 2.

Table 2. Available phases in 3 samples before ageing

Phase indication	Appearance
Al_2CuMg	Big white circular
Al_2Cu	Small white dot
Al(CuMgFe)	Small white dispersion
Al(CuMgFe)	Black dispersion
Al(CuMn)	White irregular
Al(CuMgMnFe)	White dot (found in S2 only)
Al(Cu Mg)	Black dot (found in S2 & S3)

Focusing on Sample 1 (Al-3.5Cu-1Mg-0.55Mn) we found some basic phases, the base material is alpha (α), that is the solid solution of Cu and other elements in the FCC lattice of aluminum. The θ is prominent with gray pale phase within the matrix's' phase is also seen. These phases precipitate as colonies. That's the basic difference is θ' doesn't fall as disperse phase. Both of these phases are about 10 nm on average. But θ' remains in group so they appear a little larger. Al_2Cu is the phase responsible for corroding AA2024 in susceptible environment. The presence of precipitates also confirms that the material had been precipitation strengthened by the T-3 heat treatment for the aluminum alloy [5]. Al_2Cu precipitated during the slow cooling from the homogenizing temperature [6]. Al_2CuMg is another common phase found in this alloy. It shows no change in size and distribution with increasing Cu wt.% average size of this particle up to 150 nm. They are white, irregular shape. Al–Cu–Mg containing particle or Al_2CuMg, S phase. These second-phase particles serve to strengthen the alloy through a precipitation-strengthening mechanism, which involves obstructing movement of dislocations due the presence of the second-phase particles in the alloy [6—8]. Reaction concerning S phase is-

Solid Solution-Clusters of Cu and Mg atoms. G. P(l)zones- G.P. Compounds S' (Al_2CuMg) l-S(Al_2CuMg)

When two phases jointly precipitate, they appear darker in appearance. They are mixed with Al_2Cu and Al_2CuMg. They show the same nature as separate Al_2Cu, Al_2CuMg. A second group of particles of irregular appearance, these are present on the surface as both isolated particles and clusters or clumps of several particles. In 3 samples, Al(MgCuFe) phase was found and it appears as black discrete phase. Main feature is Mn is almost nil in this phase. When Fe constituent increases, it forms another second phase particle Al(MgCuFe) which is similar to the previous one but with a larger linear black segment. As more Fe is appeared in Sample 2, black linear phases were observed. Only in Sample 2 white dots of Al(CuMgMnFe) is found. It is predicted that the base metal constituents are clustered in some places and formed these particles. When Cu wt.% is much more, it reacts with $AlMn_6$ and form a second phase particle Al(Mn Cu) they are another strengthening element. At a same time, in sample 2 and sample 3, several black dots of Al(Cu Mg) are found. These are almost similar to S phase but its appearance is black. It is inferred that increase of Cu break the phases. Also the black color may appear as Mg is deleteriously present in these black dots. When more than one phase exists coherently, it appears as dark phases in SEM. While S phase contains up to more than 1% Cu. Similar happens with the 3^{rd} and 4^{th} particles of the Table 1. Where 3^{rd} is white (Fe wt.% =0.13) but 4^{th} particle is black (Fe wt.% = .70).

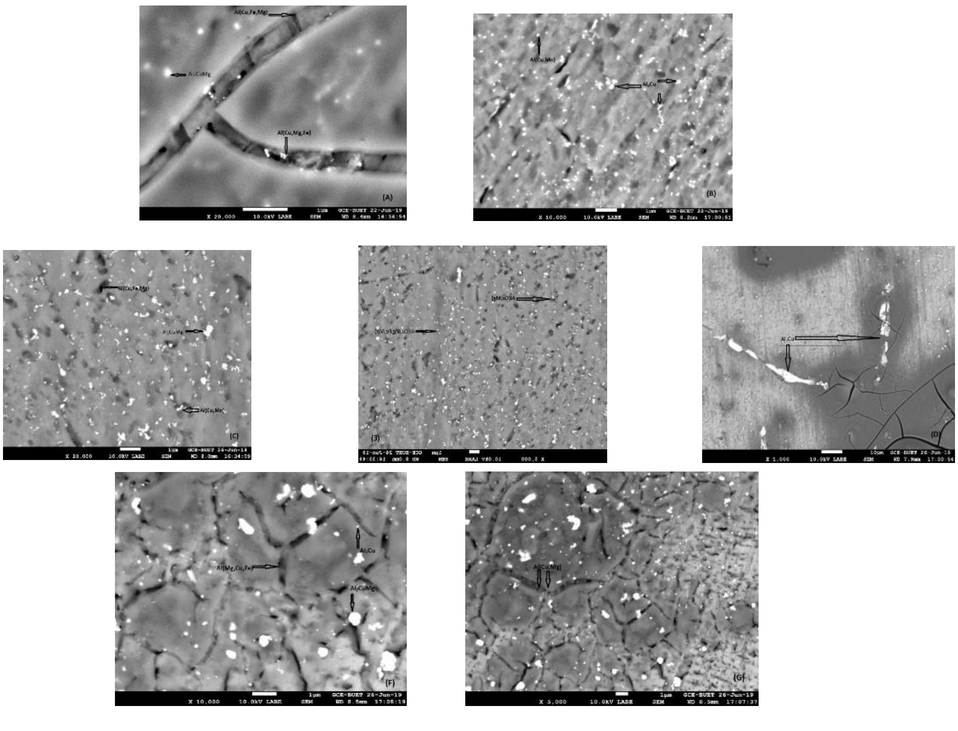

Fig. 4. SEM images of Al-3.5Cu-1Mg-0.55Mn (A & B), Al-4Cu-1Mg-0.55Mn (C, D, E), Al-4.5Cu-1Mg-0.55Mn (F & G) indicating all available phases

After Ageing (5 hours) Effect

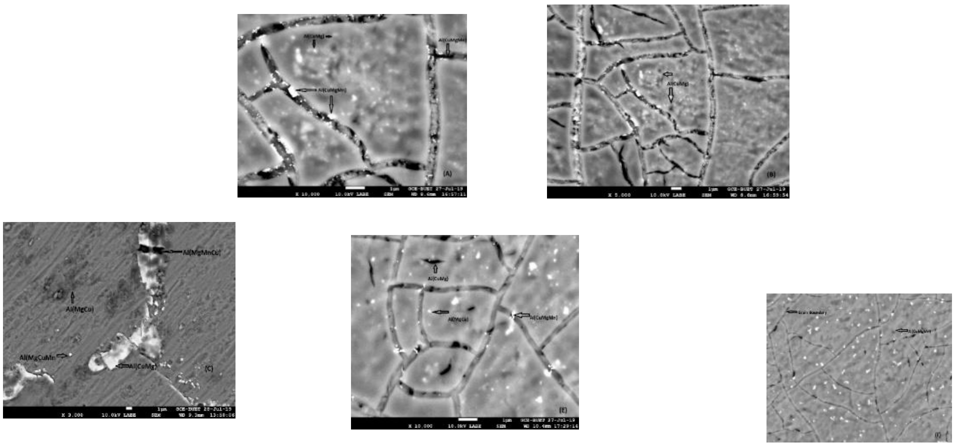

Fig. 5. SEM microstructures of Al-3.5Cu-1Mg-0.55Mn (A & B), Al-4Cu-1Mg-0.55Mn (C), Al-4.5Cu-1Mg-0.55Mn (E & F) with all available phases

The sample was aged for 5 hours in furnace. It showed some significant changes. Although no new phase appeared but the particles relaxed, so they were reshaped, their positions were altered. These coarse particles helped changing the inherent properties of the allow.as we tested hardness, it decreased due to aging. Some unknown phases which appeared before ageing are found to be vanished after ageing. Ageing left the only stable phases of materials which control the external properties. A list of available phases is provided in Table 3.

Table 3. All phases in final samples after 5 hours ageing

Phase Identifier	Appearance
Al(CuMgMn)	White circular big
Al(Mg Cu)	Very small white dispersion
Al(CuMgMn)	Black(in grains and boundaries)
Al(Cu Mg)	Black phase in grain
Al(CuMgMn)	Grain boundary phase

After analyzing the microstructure after ageing, the structure shows lack of Mn in grains. Mn has entered into the dispersed black phase. Also some of them took space in boundaries, leaving the grains empty of it. Comparing with the microstructure before ageing, few Mn was present in the grains but black phase was completely Mn free. Now it can be inferred that due to continuous heat treatment for 5 hours, slow diffusion of Mn from grain to boundary has been possible. It is assumed that lattice structure of black phase may be a bit flexible due to the continuous heating which allows Mn to reach and stay in coherent phase with Cu and Mg. Loss of Mn made the grains quite friable. Manganese has a marked strengthening effect and this is due to its solubility and the formation of several intermetallic compounds [9, 10]. During the casting of the alloy, most of the manganese remains in solution but during homogenization it combines with iron to form intermetallic compounds such as $(CuFeMn)_3$ and (CuFeMn)Al which in turn reduce the embrittling effect of iron. [11, 12] It is known that ageing reduces the internal stress and makes material stable. Long time aging can enhance mechanical properties of AA2024. Natural 5 hours aging was carried out on the samples. During this short period, only unstable phases dissolved, made the specimen homogenized. Lack of precipitating phase distribution helps the dislocation to pass easily. In fact, it increases overall ductility of the material. This the reason why hardness was a bit lower in aged samples than the quenched ones. The effect of manganese in solution is reported to retard the onset of recrystallization whereas the manganese rich intermetallic, which are associated with the sub-boundary dislocation network, inhibit grain growth [13, 14]. The size and spacing of these particles, therefore, have an important effect on the mechanical properties of the material. Iron and manganese, being transitional elements do not influence the age hardening mechanism [13]. Their resistance increases materials hardness. The effect of ageing time on hardness is shown on Fig. 6.

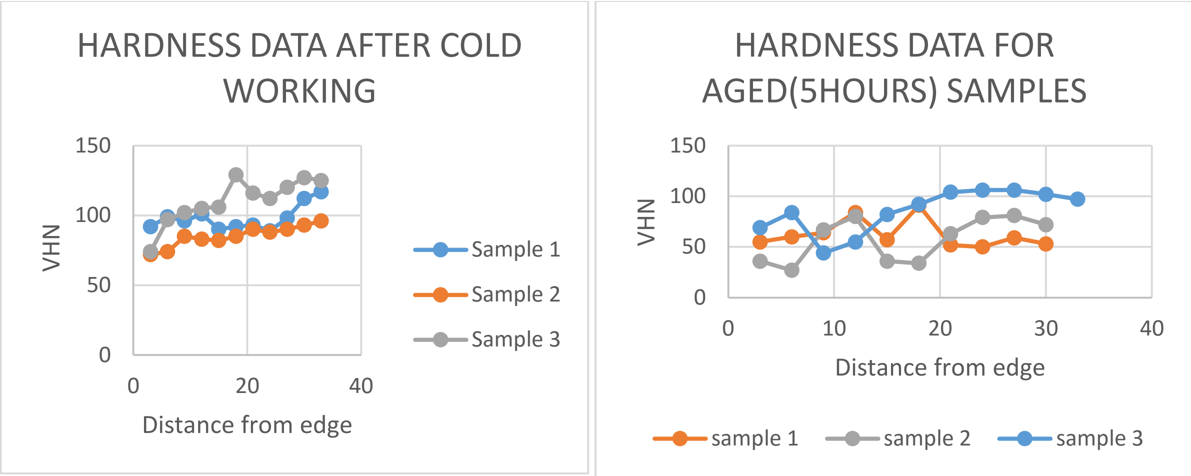

(a) AA2024 with 3.5wt.% Cu (sample 1),4wt.%Cu (sample 2),4.5wt.%Cu (sample 3) (b) AA2024 with 3.5wt.% Cu (sample 1),4wt.%Cu (sample 2),4.5wt.%Cu (sample 3)

Fig. 6. Hardness value of 3 samples (a)after cold work (b) after 5 hours ageing

Conclusion

From above experiment it is confirmed that increasing Cu wt.% helps enhancing property of AA2024 up to 4% more Cu makes the entire sample brittle. Age hardening increases mechanical properties. Long term ageing is more fruitful if better properties are about to achieve.

Acknowledgements

The authors are grateful to Bangladesh University of Engineering and Technology for providing support for the work.

References

[1] A. Guinler, Compt. Rend.' (1938), 206,1641

[2] R. Nicholson and J. Nutting, 'Phil. Mag.' (1958), 38,531

[3] V. A. Phillips, 'Acta Met’, (1973), 21,219

[4] Fundamentals of Materials Science and Engineering AN INTEGRATED APPROACH-William D. Callister, Jr. pg- 151

[5] Characterization of 2024-T3: An aerospace aluminum alloy - Zainul Huda a, ∗, Nur Iskandar Taib b,1, Tuan Zaharinie a,2

[6] Microstructural Development and Tensile Strength of an ECAP - Deformed Al-4 wt. (%) Cu Alloy,203

[7] H. Kacer, E. Atik, C. Miric, J. Mater. Process. Technol. 142 (3) (2003) 762.

[8] J. Mao, S.B. Kang, J.O. Park, J. Mater. Process. Technol. 159 (3) (2005) 314.

[9] S.J.B. Reed, Electron Microprobe Analysis and Scanning Electron Microscopy, Cambridge University Press, UK, 2005.

[10] K. R. Horn, Aluminum, Vol. 1, (1967), A.S.M. Metals Park, Ohio

[11] R. B. Ross, 'Metallic Materials Specification Handbook' (1972) SPON, London

[12] D. S. Thompson, 'Met. Trans.' (1975), 6A, 671

[13] L. F. Mondolfo, Aluminum Alloys, Vol 1 (1976) Butterworth

[14] M. V. Lancker, Metallurgy of Aluminum Alloys, (1967), Chapman Hall, London